Available online at www.sciencedirect.com
SCIENCE DIRECT®
ELSEVIER
Nuclear Instruments and Methods in Physics Research A 536 (2005) 266–272
NUCLEAR INSTRUMENTS & METHODS IN PHYSICS RESEARCH Section A
www.elsevier.com/locate/nima

The Stern–Gerlach polarized ion source for the Munich MP-tandem laboratory, a bright source for unpolarized hydrogen and helium ion beams as well ☆

R. Hertenberger*, A. Metz, Y. Eisermann, K. El Abiary, A. Ludewig, C. Pertl, S. Trieb, H.-F. Wirth, P. Schiemenz, G. Graw

Ludwig-Maximilians-Universität München, Am Coulombwall 1, D-85748 Garching, Germany

Available online 11 September 2004

Abstract

The design of our source of negatively charged, intense and brilliant DC beams of polarized hydrogen and deuterium ions was motivated by the excellent performance of the HERMES atomic beam source and the successful operation of a polarized ion source at TUNL. Deviating from their 30 K atomic beam technology we combine an 80 K atomic beam source (ABS) with subsequent ionization in an electron cyclotron resonance (ECR) plasma. In a separate unit, negative ions are obtained by successive two electron pickup from cesium in a vapour jet target. Our ABS provides a flux of 6.4×10^{16} atoms/s for hydrogen and of about 5×10^{16} atoms/s for deuterium into a compression tube of 10 mm diameter and 100 mm length. Polarized negative $\vec{D}^-/\vec{H}^-$ ion beams of about 9 μA/15 μA with an emittance of $20\,\pi$mm rad $\sqrt{\text{eV}}$ have been observed. After tandem acceleration we have polarized beam intensity of 2 μA on target of the Q3D spectrograph. The measured vector polarizations of the $\vec{D}$ and $\vec{H}$ ion beams are 72% and 67%, respectively, in accordance with expectations from source operation data. Using an external gas inlet for the ECR region, intense beams of unpolarized $^1H^-$, $^2D^-$, $^3He^-$, and $^4He^-$ ions are obtained.

PACS: 29.25.Lg; 29.25.Ni

Keywords: Polarized hydrogen; Deuterium ion beam; Helium ion beam

1. Introduction

In storage rings, internal polarized hydrogen gas targets have been pioneered by the use of high-intensity Stern–Gerlach atomic beam sources (ABS). For the HERMES target at the DESY

☆ Supported by MLL, DFG and BMBF.
*Corresponding author.
E-mail address: ralf.hertenberger@physik.uni-muenchen.de (R. Hertenberger).

0168-9002/$ - see front matter © 2004 Elsevier B.V. All rights reserved.
doi:10.1016/j.nima.2004.08.083

electron storage ring HERA [1] and for the PINTEX target at the IUCF cooler ring [2] the ABS are optimized with respect to particle flux. They are operated at nozzle temperatures near 80 K. Optimized vacuum systems with four differentially pumped sections and arrays of up to 6 permanent sextupole magnets of FeNdB [3–5] are used as a spin filter and produce electron polarized atomic beams. The electron polarization is converted into nuclear polarization by adiabatic radiofrequency transitions, which interchange the populations between two selected Zeeman-splitted hyperfine levels. Fluxes of 7×10^{16} H/s have been reported [4] and recently 12×10^{16} H/s [5].

Sources for polarized beams of positively or negatively charged hydrogen and deuterium ions $\vec{H}^{\pm}$ or $\vec{D}^{\pm}$ require density optimized atomic beams at the position of ionization. They typically use ABS operated with nozzle temperatures near 30 K and respective slow atomic beam velocities [6]. For the production of negatively charged polarized ion beams, we use for the first time the 80 K ABS-technology with FeNdB magnets in combination with ionization in an electron cyclotron resonance (ECR) plasma, followed by subsequent double electron pickup in a dense cesium vapour jet. This scheme is based on the successful operation of a source at TUNL which, however, uses the 30 K technology and conventional sextupole magnets [6–8], and a rather compact design of the ionization and charge exchange region. We expected, the higher atomic flux and the better emittance of the 80 K ABS to compensate for the density reduction due to higher beam-velocity.

In comparison to polarized hydrogen ion sources of highest beam intensities, the combination of ABS, electron cyclotron ionizer and cesium vapour target is attractive because of its versatility. The use of subsequent adiabatic RF-transitions allows to produce any kind of vector or tensor polarization both for $\vec{H}$ and $\vec{D}$ ion beams. Background effects dilute the polarizations to only 80% of the ideally expected values. The negatively charged ion beams out of the source have intensities near 10 μA, good emittance and are well suited for tandem accelerators like the Munich MP-tandem. Furthermore, this facility is in use as a reliable source of unpolarized hydrogen, deuterium, ^{3}He or ^{4}He ion beams of excellent brilliance.

2. Atomic beam source

A vertical section of the ion source is shown in Fig. 1. The Stern–Gerlach part consists of four differential pumping stages. Section 1 houses the dissociator [9], Sections 3 and 4 the Stern–Gerlach sextupole magnets and the adiabatic RF-transitions. The additional pumping in stage 2 reduces the scattering of the beam from residual gas, and enhances the beam intensity by about 20%. Molecular hydrogen gas is dissociated by means of electron impact in a cold plasma driven by a high-frequency circuit. An atomic jet is created by adiabatic expansion into the vacuum of chamber 1 out of an aluminum nozzle that is cooled to 80 K. Two apertures determine the part of the jet which enters the sextupole magnet system. Four Stern–Gerlach magnets built from permanently magnetized FeNdB material are used for separation with respect to electron spin. The electron polarization is transferred to nuclear polarization using adiabatic RF-transitions. They induce the selective interchange of two hyperfine substate populations.

At the working point the hydrogen flow rate through the dissociator is 2.2 mbl/s at 350 W of 13.5 MHz RF-power and at a degree of dissociation of $77 \pm 5\%$. For deuterium the working point is 1.5 mbl/s at 290 W with a similar degree of dissociation. Through the entrance of the ECR ionizer, an aperture of 10 mm diameter, the ABS provides atomic beam intensities of 6.4×10^{16} atoms/s for hydrogen and of about 5×10^{16} atoms/s for deuterium [10].

3. ECR ionizer and positive ion beam

In an ECR plasma, the atomic beam is ionized by electron impact with an efficiency of a few percent. Two pancake coils with magnetic flux guidance provide the axial magnetic mirror field with a minimum of 87.5 mT located in between the maxima of 160 and 140 mT. A standard waveguide

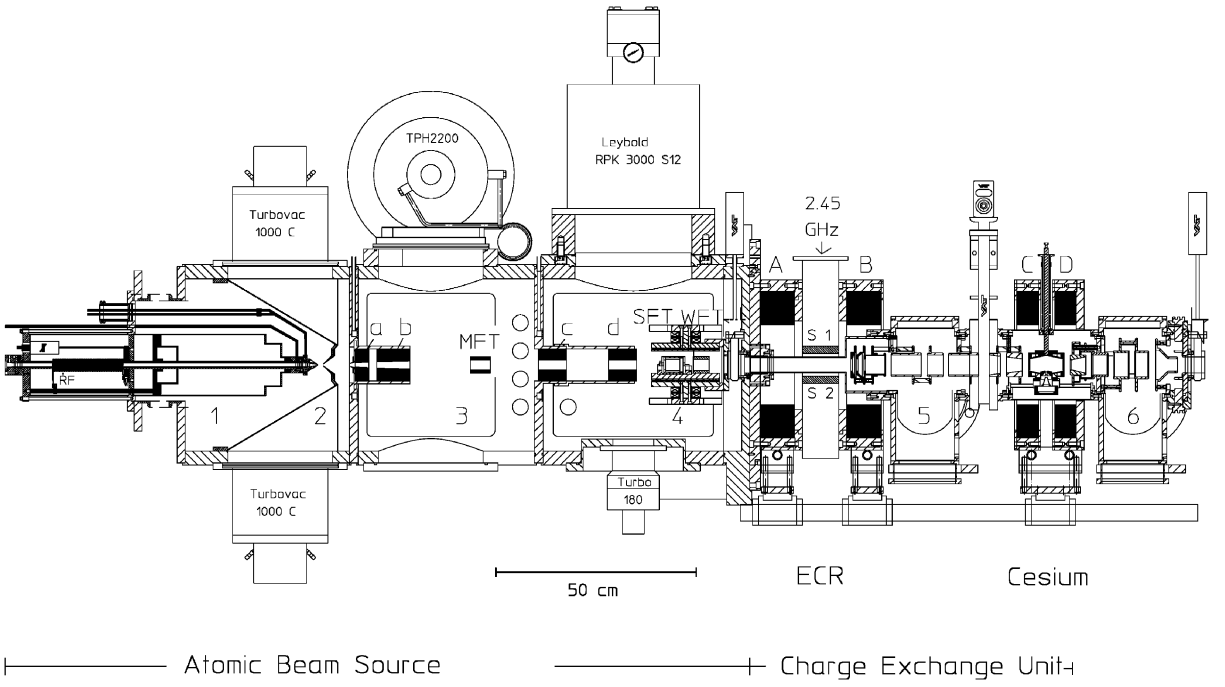

Fig. 1. Vertical section of the ion source: The Stern–Gerlach ABS consists of four differential pumping stages (1–4), four permanent sextupole magnets (a–d), adiabatic radiofrequency transitions (MFT,SFT,WFT) and the dissociator in vacuum chamber 1. For ECR ionization two pancake coils (A,B) produce an axial magnetic mirror field and six permanent FeNdB dipoles S1–S6 the radial magnetic field for plasma confinement. Shown are S1 and S2 only which are placed within the waveguide. The plasma within the RF-waveguide couples directly to the 2.45 GHz RF-field. Two pancake coils C and D provide a magnetic holding field near 100 mT to preserve polarization during successive pickup of two electrons in cesium vapour. The positive and negative ions are transported by a system of electrostatic electrodes.

for RF-power of 2.45 GHz is used as field applicator to the plasma. A cylindrical pyrex vessel insulates the plasma from the waveguide. Two circular 40 mm holes in the small sides of the wave guide define its position. Close to the 875 G contour the plasma burns at the location of a maximum of the electric RF-field of the 2.45 GHz H_{10} wave. In this way the electric RF-field direction is perpendicular to the axial magnetic mirror field and accelerates electrons in phase with their cyclotron frequency of 2.45 GHz at 87.5 mT. Inspecting the Bremsstrahlung spectrum out of the pyrex tube a maximum value for the electron energies of about 20 keV was observed. The coupling of the RF-wave to the plasma is effective, for best operation a power of 27 W is sufficient. The sextupole field for radial confinement of the plasma is provided by six dipole magnets of FeNdB. Two of them are located inside the waveguide. No absorption of the RF-wave or overheating of the magnets has been observed. For stable plasma operation, nitrogen gas is introduced into the ECR volume by a separate inlet. The amount of nitrogen necessary to sustain the plasma corresponds to about 60% of the total plasma current including the atomic beam.

The positive ion beam is transported by an electrostatic lens system. The axial magnetic fields in the ECR and in the cesium charge exchange regions provide some additional guidance. Because of technical reasons, mainly with respect to the ease of maintenance of the source, we decided to have the ECR and the cesium region well separated by a valve in between. In this way we do not use the ion optical advantage of a continuous magnetic field from the ECR to the cesium region. A large inner diameter of 30 mm was chosen for the plasma and the extraction

electrodes to avoid collisions of the atomic beam with the electrodes. The part of the atomic beam that is not ionized in the ECR volume should fly unhindered into more downstream regions, where the pumping is most effective and where back-diffusion of recombined molecules into the plasma region is decreased. Hereby, depolarized background is reduced. The beam is extracted from the plasma in two steps using three electrodes. They are followed by an Einzellens. The ion beam is then focused into the cesium target by two deceleration electrodes. The negative ion beam is transported by four electrodes and is accelerated to an energy of 10 keV at the end of the source. After a distance of 15 cm, its emittance is limited by three apertures of 10, 5 and 10 mm in diameter with relative distances of 6.5 cm to $\varepsilon = 20\,\pi\text{mm mrad}\sqrt{\text{eV}}$ before it enters the Wien filter used for spin rotation.

4. Cesium vapour jet target

The main components of the cesium vapour jet target are a cesium reservoir, which is heated up to 310 °C by means of 120 W of heating power, an expansion nozzle, a baffle, a water cooled condensation surface kept at a temperature of 35 °C and a wire-mesh to guide the recirculation of condensed liquid cesium back into the cesium reservoir. At the reservoir temperature of 310 °C the vapour pressure of cesium is about 3 mbar. Besides the heated reservoir and the nozzle all surfaces are kept at 35 °C, which reduces the vapour pressure of cesium at these surfaces to 5×10^{-6} mbar. By expansion of the cesium vapour through the slit nozzle a supersonic jet is formed. About 30% of the vapour passes the baffle and enters the charge exchange region. The central part of the cesium jet crosses the ion beam. Here occurs the charge exchange into negative ions by successive pickup of two electrons. Then the jet hits the 35 °C surface where the cesium atoms condensate into the liquid phase and recirculate into the heated cesium reservoir. The part of the jet that hits the baffle recirculates immediately into the heated reservoir. The baffle is in good thermal contact with the 35 °C surface. According to Ref. [11], the double charge exchange in the cesium jet saturates at a cesium area density of 10^{15} atoms/cm^2. To maintain the polarization of the ion beam the charge exchange occurs in an axial holding field of about 100 mT. We measured at a kinetic energy of 400–500 eV/nucleon the efficiency for double charge transfer $D^+ \rightarrow D^-$ to 22% [12].

5. Negative ion beams

Fig. 2 shows an intensity measurement of negative polarized deuterium ion beam mass analyzed by a Wien filter. The beam intensity is shown as a function of the temperature of the dissociator nozzle. The almost linear decrease in beam intensity is due to the convolution of the temperature-dependent beam profile, the transmission function through the sextupoles and the velocity dependence of the ionization efficiency in the ECR ionizer.

The maximum D^- beam intensity of 13.5 μA in three hyperfine substates does not saturate at a temperature of 80 K, but lower nozzle temperatures are presently not accessible. The D^- beam

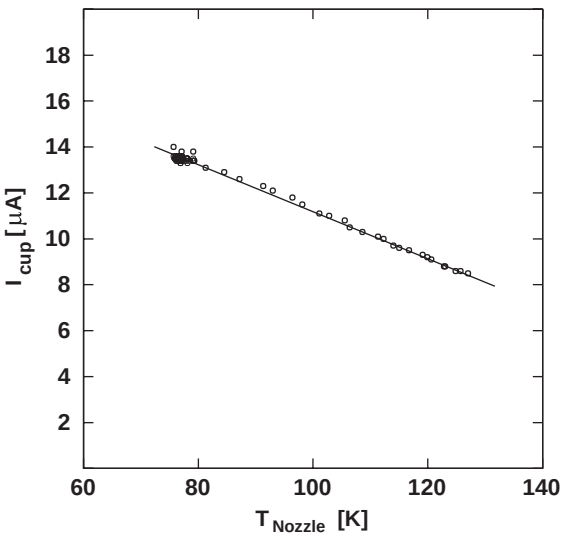

Fig. 2. Intensity of the polarized negative deuterium ion beam (out of three hyperfine substates) as a function of the temperature of the dissociator nozzle.

intensity corresponds to 9 μA of vector polarized ion beam out of two hyperfine substates with an emittance of about $\varepsilon = 20\,\pi$mm mrad $\sqrt{\text{eV}}$.

After acceleration by the Munich tandem accelerator, polarized beam intensities of 2 μA are available for $\vec{\text{H}}$ and $\vec{\text{D}}$ ion beams.

6. Polarization

To tune the adiabatic RF-transitions, elastic scattering reactions are performed at the Q3D magnetic spectrometer. Countrates above 5 kHz are achievable at target area densities of a few mg/cm^2 using reactions with cross sections above 10 mb/sr. This allows on-line tuning of the adiabatic RF-transitions. For deuterons, the elastic scattering reaction 22 MeV ^{65}Cu($\vec{\text{d}}$, d$_0$) was used at the scattering angle of 75°. It has a vector analyzing power of $A_y = -0.70$ and a low value for the tensor analyzing power of about $A_{yy} = 0.25$. For protons, we used the elastic scattering reaction 21.1 MeV ^{12}C($\vec{\text{p}}$, p$_0$) with an analyzing power of $A_y = 0.563$ at 75°. Vector polarizations of 72% and 67% have been observed for accelerated deuterons and protons, respectively.

The adiabatic RF-transition units are similar in construction to those used in the HERMES experiment. For these transitions efficiencies near 0.99 have been observed. We expect similar numbers for our facilities. Then the ion beam polarization depends predominantly on incomplete hyperfine state separation by the sextupole system, on remaining hyperfine coupling at the location of ionization and charge exchange and on ionization of unpolarized residual gas.

The sextupole hyperfine state separation is obtained from ray-tracing calculations, the hyperfine coupling is relevant for hydrogen only, for deuterium the holding fields are sufficient.

For hydrogen the hyperfine-states $|2>$ and $|4>$ are linear combinations of strong field configurations, the mixing angle θ is determined by $\cos(2\theta) = x/\sqrt{1+x^2}$ with $x = B/B_c$ and $B_c = 50.7$ mT. Thus hyperfine-states $|4>$ and $|2>$ have proton polarizations of $\pm\cos 2\theta$, at the ECR field of 87.5 mT this is ±0.865. Accordingly a beam out of states $|1>$ and $|4>$, both equally populated, or out of states $|2>$ and $|3>$ has a proton polarization of $\pm(1+\cos(2\theta))/2$ or ±0.933. In the ionization process the electron is removed in a sudden process, thus the proton spins are spectator and the polarization remains.

Adding an unpolarized cesium electron to a spin up proton gives hydrogen atoms in states $|1>$ and $|4>$, and in finite holding field also in state $|2>$. In a vapour jet, the second electron is added after some time, a number of hyperfine-rotations has taken place, thus phases average out, and the proton polarization in the negative ion results as $(1+\cos^2(2\theta))/4$. Multiplying this with the initial proton polarization yields $0.99 \times 0.93 \times (1+\cos^2(2\theta))/4$ or 0.815, if the magnetic holding field in cesium has the same value as the field in the ECR region.

Comparison with the measured 0.67 proton polarization observed for the high-energy beam, yields a 15% dilution of the polarization, which is expected to result mainly from residual gas ionization. The observed value of 0.72 for the deuterium polarization is consistent with this value of dilution and with calculated values around 0.93 for two state operations due to incomplete hyperfine-separation in the second part of the sextupole system.

7. Unpolarized ion beams

Meanwhile, the source is used extensively for unpolarized H, D and ^{3,4}He ion beams. For unpolarized operation, a separate gas inlet into the ECR area is used. Beam intensities above 50 μA after the Wien filter are achievable for hydrogen and deuterium and intensities around 10 μA for He ion beams. For reasons of γ-ray buildup and radiation load of the accelerator, we restricted so far the intensity of accelerated H and D ion beams to 3 μA on target. Accelerated ^{3,4}He ion beams of up to 1 μA were observed.

Of all the unpolarized experiments, the most challenging in regard to beam quality is the ion nanoscope SNAKE, a superconducting quadrupole triplet for the production of accelerated ion beams with a sub-μm focus. It is designed to resolve nano structures in applied and material

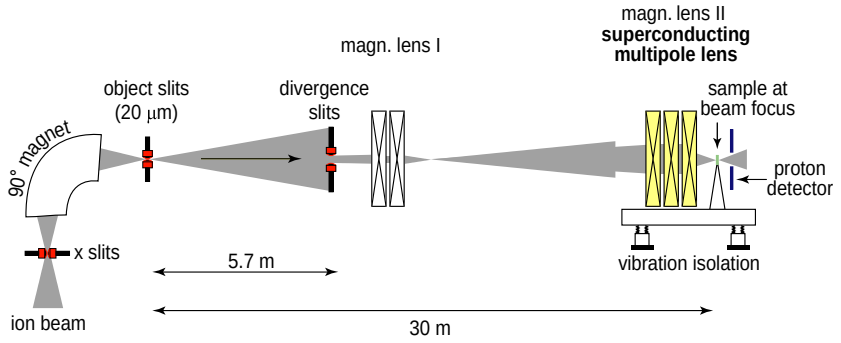

Fig. 3. Ion optics for the SNAKE experiment.

science. One goal was to detect and localize hydrogen in artificially grown chemically vapoured diamond (CVD). The hydrogen could be localized for the first time by correlated detection of two protons in p–p scattering by P. Reichart and G. Dollinger from T.U. München. An area of 70 μm by 7 μm was scanned with the hydrogen beam focused to a spot size of about 1.5 μm × 0.7 μm. Fig. 3 gives a survey of the ion optics. The slits after the 90° bending magnet are closed to 20 μm. They define together with the divergence slits the accepted phase space. The divergence slits are opened in x to 1800 μm and in y to 1200 μm. The corresponding phase space is about 225 $\mathrm{mm^2\,mrad^2\,eV}$. Unpolarized negative hydrogen beam with an intensity of almost 100 μA after the source was necessary to supply 80 pA of ion beam on target with a brilliance of $3.1\times10^{-14}\,\mathrm{A/(mm\,rad\,\sqrt{eV})^2}$. For the first time hydrogen enrichment in the grain boundaries of artificially grown CVD could be detected, see Fig. 4 and Ref. [14].

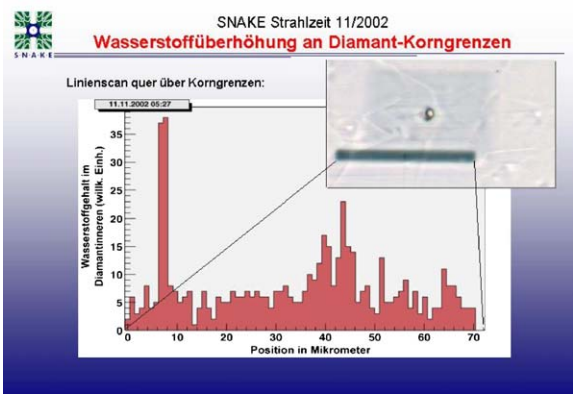

Fig. 4. Localization of hydrogen in the grain boundaries of artificially grown CVD. The right upper picture shows a microscopic optical picture of the surface of the diamond with three grain boundaries. The dark area corresponds to a size of 70 μm × 7 μm. It was scanned by the hydrogen ion beam with a focus size of approximately 1.5 μm × 0.7 μm. The y-axis shows the hydrogen content in arbitrary units. A line from p–p scattering shows up at 7 μm and two lines around 40 μm. The latter two correspond to a grain boundary that is tilted against the surface with an angle differing from 90°.

8. Summary

The polarized hydrogen source is used in routine operation since 2001. Its operation is reliable over weeks with intensities of vector polarized deuterium and hydrogen beams between 1–2 μA on target and with nuclear polarization near 70%. During twenty-five weeks of beamtime, with data taking periods of typically two weeks, we measured nuclear excitation spectra (with energy resolution of up to 4 keV FWHM) and obtained angular distributions of $\mathrm{d}\sigma/\mathrm{d}\Omega$ and A_y for more than twenty different nuclear reactions. Maintenance is routinely performed after five weeks of running with a cesium consumption of 20 g. Multinucleon transfer reactions as $^{198}\mathrm{Hg}(\vec{\mathrm{d}},\alpha)^{196}\mathrm{Au}$ [13] for the study of supersymmetry in heavy odd–odd nuclei profit considerably from the increase in beam intensity and beam quality.

References

[1] A. Nass, et al., Nucl. Instr. and Meth. A 505 (2003) 633.
[2] T. Wise, A.D. Roberts, W. Haeberli, Nucl. Instr. and Meth. A 336 (1993) 410.
[3] P. Schiemenz, A. Ross, G. Graw, Nucl. Instr. and Meth. A 305 (1991) 15.
[4] M. Mikirtytchiants, et al., Proceedings of the Ninth International Workshop on Polarized Sources and Targets, Nashville, TN, 2001, p. 47.
[5] A. Zelenski, International Workshop on Polarized Sources and Targets, Novosibirsk, September 2003.
[6] T.B. Clegg, et al., Nucl. Instr. and Meth. A 357 (1995) 200.
[7] T.B. Clegg, W.M. Hooke, E.R. Crosson, A.W. Lovette, H.L. Middleton, H.G. Pfutzner, K.A. Sweeton, Nucl. Instr. and Meth. A 357 (1995) 212.
[8] E.R. Crosson, T.B. Clegg, H.J. Karwowski, S.K. Lemieux, Nucl. Instr. and Meth. A 310 (1991) 703.
[9] K. El Abiary, Diploma Thesis, LMU, München, 1996.
[10] R. Hertenberger, et al., Rev. Sci. Instr. 69 (2) (1998) 750.
[11] A.S. Schlachter, et al., Phys. Rev. A 22 (6) (1980) 2494.
[12] C. Pertl, Thesis, LMU, München, 2000.
[13] A. Metz, et al., Phys. Rev. Lett. 83 (1999) 1542;
A. Metz et al., Phys. Rev. C 61 (2000) 064313–1.
[14] P. Reichart, G. Dollinger, et al., Nucl. Instr. and Meth. B 567 (2003) 3.